Surface modification and cellular uptake evaluation of Au-coated Ni80Fe20 nanodiscs for biomedical applications

Barrera, Gabriele; Serpe, Loredana; Celegato, Federica; Cösson, Marco; Martina, Katia; Canaparo, Roberto; Tiberto, Paola. Surface modification and cellular uptake evaluation of Au-coated Ni80Fe20 nanodiscs for biomedical applications. INTERFACE FOCUS. 6 (6) pp: 20160052-20160057. DOI: 10.1098/rsfs.2016.0052

Surface modification and cellular uptake evaluation of Au-coated $Ni_{80}Fe_{20}$ nanodisks for biomedical applications

Gabriele Barrera[1], Loredana Serpe[2], Federica Celegato[1], Marco Coïsson[1], Katia Martina[2], Roberto Canaparo[2], Paola Tiberto[1]

[1]INRiM, Nanoscience and Material division, I-10135, Torino, Italy

[2]University of Turin, Dept. of Drug Science and Technology, I-10125, Torino, Italy

Abstract

A nanofabrication technique based on self-assembling of polystyrene nanospheres is used to obtain magnetic $Ni_{80}Fe_{20}$ nanoparticles with a disk shape. The free-standing nanodisks (NDs) have diameter and thickness of about 630 nm and 30 nm respectively. The versatility of fabrication technique allows to cover the NDs surface with a protective gold layer with a thickness of about 5 nm. Magnetization reversal has been studied by room-temperature hysteresis loop measurements in water-dispersed free-standing nanodisks. The reversal shows zero remanence, high susceptibility and nucleation/annihilation fields due to spin vortex formation. In order to investigate their potential use in biomedical applications, the effect of nanodisks coated with or without the protective gold layer on cell growth has been evaluated. A successful attempt to bind cysteine-fluorescein isothiocyanate (FITC) derivative to the gold surface of magnetic NDs has been exploited to verify the intracellular uptake of the nanodisks by cytofluorimetric analysis using the FITC-conjugate.

Keywords

Self-assembly, Magnetic Nanodisks, Magnetization reversal, Cytoxicity

Introduction

In the last years, magnetic nanoparticles have been widely studied to be exploited in biomedicine with different purposes [1,2]. However, recent developments in this field have brought an increased interest in the synthesis and characterization of new types of magnetic nanoparticles. In particular, the ability to control size, shape, and composition of magnetic nanoparticles can provide flexibility for biomedical applications such as DNA separation, cell labeling, magnetic resonance imaging MRI, drug delivery, and magnetic hyperthermia [3-6].

Magnetic nanoparticles require a surface treatment or coating to be exploited in biomedical applications to protect them from oxidation or redissolution, to prevent the aggregation among nanoparticles, to increase their biocompatibility and their affinity for other molecules to further extend their functionalities [7-8].

The well-known optical properties, surface chemistry and biological reactivity of gold have made this element widely used as coating material for magnetic nanoparticles. Gold coating improves not only the stability of the magnetic particles but also provides a useful surface to bond chemical and biological entities maintaining unaltered the magnetic behavior of the particles [9]. However, the direct chemical coating of

magnetic particles with gold results to be difficult, due to the dissimilar nature of the two surfaces, consequently nowadays different routes are investigated [10-13].

Usually, the conventional methods to synthesize magnetic nanoparticles are via chemical routes [14,15]. Despite they are low-cost methods allowing to synthesize high volumes of nanoparticles, their major drawback is the difficulty to obtain monodispersed dimensions leading to different and not easily predictable magnetic behavior. To overcome such limits, recent studies have demonstrated the viability to use top-down approaches to fabricate specifically designed magnetic nanoparticles [16-18].

In this work, magnetic $Ni_{80}Fe_{20}$ nanoparticles having disk shape have been synthesized and directly coated by a gold layer by means of a bottom-up self-assembling nanolithography process assisted by polystyrene nanospheres, that it is widely considered as a valid alternative to conventional lithographic techniques (i.e. optical and electron) [19,20].

Nanoparticles having disk shape offer some advantages in biomedicine compared to the spherical ones; in particular, they adhere more effectively to the biological substrate [21], exhibit a higher margination propensity [22] and accumulate more efficiently in the organs [23]. These results indicate their potential use for the systemic delivery of drugs, in biomedical imaging and in hyperthermia treatments.

The magnetic $Ni_{80}Fe_{20}$ alloy and the size of nanodisks were chosen to induce a vortex-state spins arrangement in each nanostructure. This magnetic arrangement possesses the peculiar property of a zero-remanence as in the case of superparamagnetic nanoparticles, but compared to them it has a higher magnetic saturation and susceptibility as well as the appearance of hysteresis at high fields [24]; these peculiar properties make the nanoparticles with magnetic vortex behavior a promising candidate for diverse biomedical applications, especially in cancer cells detection and destruction [6,25,26].

A thorough knowledge on the potential cytotoxicity and the interaction with cells of magnetic nanodisks is crucial for their biomedical applications [27]; therefore a detailed study about the effects on cell viability is essential. In particular, in this paper, a comparative cytotoxicity study of Au-coated and bare $Ni_{80}Fe_{20}$ nanodisks at different concentrations has been performed on HT-29 human colorectal adenocarcinoma cells. Subsequently, a functionalization of gold surface of coated nanodisks is performed with a cysteine-fluorescein isothiocyanate (FITC) derivative in order to induce a random fluorescence and use them to evaluate the intracellular uptake.

Materials and Methods

Nanofabrication process of nanodisks

Au-coated ferromagnetic nanodisks (Au-NDs) are fabricated by exploiting polystyrene nanospheres (PN) lithography [Tiberto dischi]. The multi-steps process is schematized in Fig. 1 (note that is a not-to-scale scheme). In the first step, Fig. 1(a), a Si substrate is coated by a layer of optical resist; on top of this an $Au/Ni_{80}Fe_{20}/Au$ tri-layer film is sputtered each layer having thickness of 5 nm/30 nm/5 nm respectively. The gold layer deposited by sputtering both before and after the magnetic material deposition has the purpose of coating the magnetic $Ni_{80}Fe_{20}$ core with biocompatible surface and for subsequent bio-functionalization. Then, an almost hexagonal-close-packed monolayer of polystyrene nanospheres (starting diameter 800 nm) is deposited by floating technique onto the tri-layer, (as illustrated in Fig. 1(b)). In the third step, the PNs diameter is reduced by plasma etching in Ar^+ in order to expose a portion of the tri-layer surface among

PNs, see Fig. 1(c). In the present case, at this step, the etching time has been chosen in order to obtain the final PNs diameter of about 630 nm. In the step shown in Fig. 1(d), the polystyrene nanospheres are used as a hard mask for sputter etching with Ar^+ ions used to remove the exposed tri-layer material among the PNs, as. The subsequent removal of the PNs mask (lift-off) by sonication in deionized water leaves an array of ordered nanodots on the surface of the resist layer having the same composition and thickness as the starting continuous tri-layer film (Fig. 1(e)). In the last step of fabrication process, the underlayer of resist is dissolved in acetone and ends up with detached freestanding Au-NDs (Fig. 1(f)) dispersed in the solvent. Through several rinsing with deionized water assisted by magnetic separation using a field gradient, the Au-NDs were cleaned by acetone and in the end dispersed in deionized water.

In order to evaluate the effect of Au layer, the same process has been used by depositing only the $Ni_{80}Fe_{20}$ film (t = 30 nm) in place of the tri-layer shown in Fig. 1a. In this case, the final sample is therefore constituted by bare $Ni_{80}Fe_{20}$ magnetic nanodisks (bare-NDs) dispersed in water.

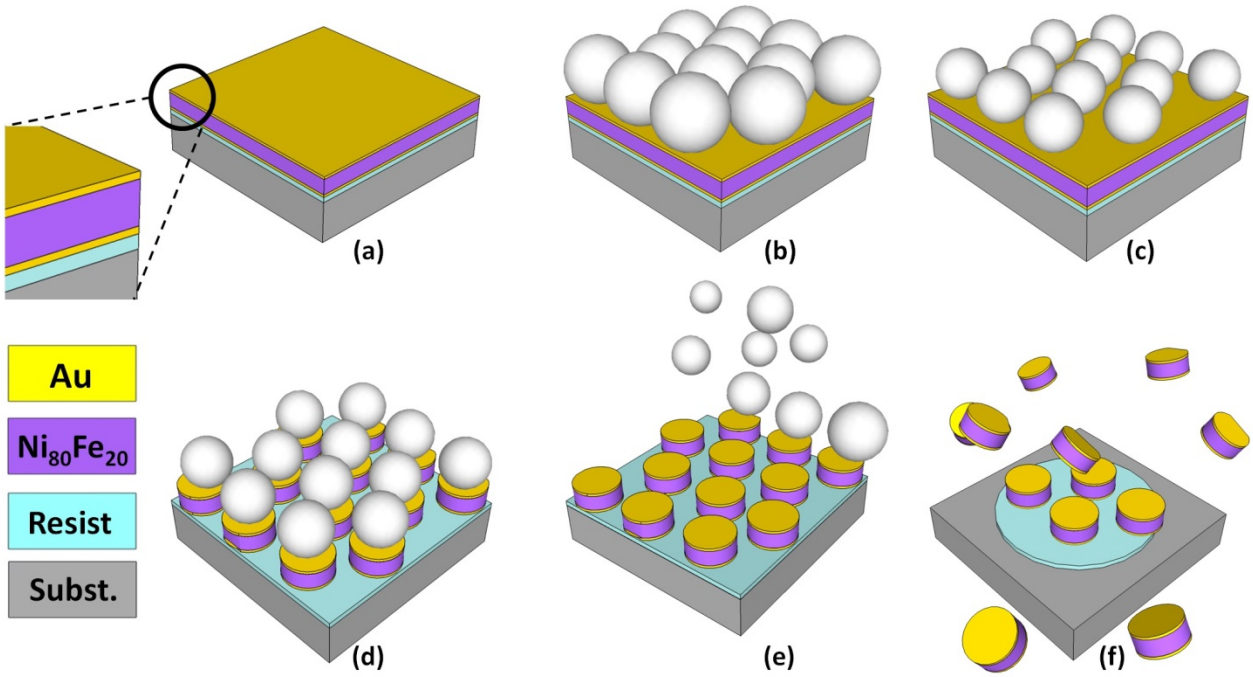

Figure 1. Schematic description of the nanofabrication process: (a) sputter deposition of an Au/$Ni_{80}Fe_{20}$/Au tri-layer (thickness 5 nm/30 nm/ 5 nm); (b) deposition of a monolayer of polystyrene nanosphere (starting diameter 800 nm); (c) plasma etching in Ar to reduce PNs diameter; (d) sputter etching to remove tri-layer among spheres; (e) spheres removal by sonication; and (f) chemical dissolution of resist underlayer resulting in disks detachment from the substrate.

Morphological and magnetic characterization

Hysteresis loops at room-temperature have been measured on bare or Au-coated nanodisks in water solution by using a vibrating sample magnetometer (VSM) in the magnetic field range ±1500 Oe. The Au-NDs morphology was examined by scanning electron microscopy (SEM) equipped with a STEM (Scanning Trrasmition Electron Microscopy) detector. A drop of the Au-NDs suspended in water has been placed on a standard copper grid, followed by drying.

Functionalization of nanodisks with FITC

2.5 mg of cysteine (0.015 mmol) and 3 mg of FITC (0.077 mmol) have been dissolved in 1mL of DMSO/0.1M phosphate-buffered saline (2:1) and left under shaking 4 hours. 27 µl of the solution has been transferred

and added to a 1mL of nanodisks suspension (7.74 x 10^8 ea ml^{-1}) in 1mL of DMSO/0.1M phosphate-buffered saline (2:1) and incubated overnight. The final nanodisks/FITC have been washed 2 times with DMSO (1mL) and 8 times with 0.1M phosphate-buffered saline.

Biological assays

1. Cell line and culturing

The HT-29 human colorectal adenocarcinoma cell line (ATCC, Rockville, MD, USA) has been cultured in Minimum Essential Medium Eagle (EMEM) supplemented with 2 mM L-glutamine, 100 UI/mL penicillin, 100 μg/mL streptomycin and 10% fetal bovine serum (Sigma Aldrich, St Louis, MO, USA). Cell lines have been kept in a humidified atmosphere of 5% CO_2 air at 37°C.

The effect that nanodisks with and without the protective gold layer had on HT-29 cell growth has been evaluated using a WST-1 cell proliferation assay (Roche Applied Science, Penzberg, Germany). 1.5 × 10^3 HT-29 cells have been seeded in 100 μL of growth medium in replicates (n = 8) in a 96-well culture plate. After 24 h of cell growth, the medium has been removed and the cells incubated with experimental media of differing nanodisk concentrations (0.1, 1.0, 10.0 and 50 μg/mL). The WST-1 reagent (Roche Applied Science) (10 μL/100 μL) has been added, at 24, 48 and 72 h, and plates have been incubated at 37°C in 5% CO_2 for 90 min. Well absorbance was measured at 450 and 620 nm (reference wavelength) in the microplate reader Asys UV340 (Biochrom, Cambridge, UK).

2. Flow cytometric analysis

Analysis of nanodisk cellular uptake has been carried out on C6 flow cytometry equipment (Accuri Cytometers, Milano, Italy). Briefly, 1 x 10^5 cells have been plated in 6-well culture plates and incubated with FITC conjugated gold nanodisks (10 μg/mL) for 1, 8 and 24 h. Cells have been detached after each incubation period using a 0.05% trypsin-0.02% EDTA solution and re-suspended in 500 μL phosphate buffered solution. They have been then run on the C6 flow cytometer, which considered 10,000 events, using 488 nm excitation to measure the intracellular nanodisks. Intracellular fluorescence is expressed as integrated median fluorescence intensity (iMFI). This is the product of the frequency of cells that are positive to FITC conjugated nanodisks and the median fluorescence intensity of the cells.

Results and Discussion

The nanospheres lithography used to synthetize the bare and Au-NDs (Fig. 1) comes out as an easy-to-use and low-cost method to nanostructure thin films. The major drawback of this technique is normally the lack of long range order and the formation of some defects in the array in comparison to similar arrays obtained by means of optical or electron conventional lithographic processes [28]; however, in this context such limits are overcome by the fact that the final samples consist of free nanodisks detached from the substrate and dispersed in liquid solution (Fig 1(f)), therefore the actual ordering of the nanodisks on the substrate has not relevance on the final product.

On the other hand, the nanospheres lithography offers higher-resolution patterning than conventional optical techniques maintaining the same parallel writing method where the whole pattern is obtained simultaneously using the nanospheres as a hard mask dictating the features to be reproduced (Fig. 1(d)). Therefore, this parallel lithography process is fast and allows a wide surface coverage resulting in a promising, versatile and low cost method for nanostructuring multilayer thin films producing ordered arrays of dots (Fig. 1(e)). Depending on the available experimental setup, the final samples can be patterned by nanospheres lithography over surface areas from square millimeters to square centimeters [29].

In order to evaluate the packing density (η, fraction of surface area occupied by dots with respect to the whole substrate area) of the obtained dots array and consequently their area number density (ρ), some SEM images (with field of view of 37 x 32 μm^2) were taken in different regions of a sample having dots still attached on the substrate (as shown in Fig. 1(e)), resulting in $\eta = 0.62$ and $\rho = 1.2 \times 10^8$ dots/cm^2 respectively. Given the size of Si substrate used to fabricate both bare and Au-NDs samples is 2.54 x 2.54 cm^2, the total number of nanodisks in each sample is about of 7.74×10^8.

In addition, it is worth mentioning that, this fabrication process does not allow a complete Au-coating of the $Ni_{80}Fe_{20}$ magnetic core because the lateral surface of the dots remains uncovered, as shown in Fig. 1(f), in particular only 91.5 % of the total surface area of nanodisks is coated by the gold layer.

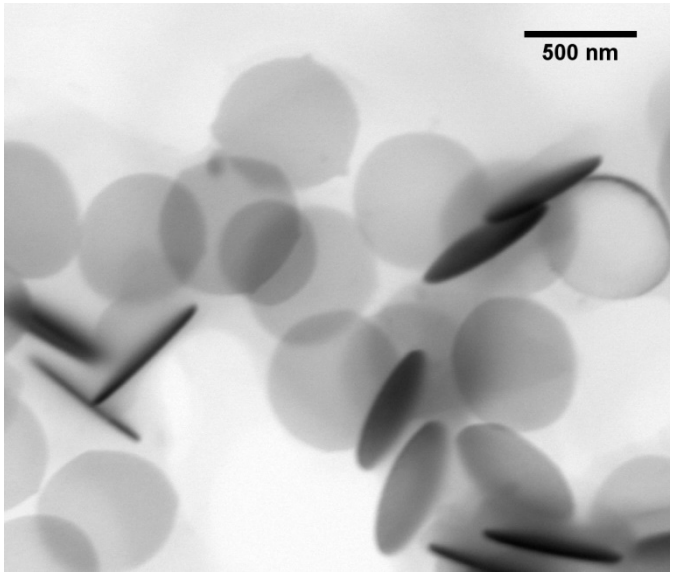

Figure 2. SEM image of free-standing Au-NDs placed on a standard copper grid.

A drop of solution was placed on a standard copper grid in order to investigate the morphology of the as-fabricated Au-NDs by SEM equipped with the STEM detector, Fig. 2. As expected, a disk shape with a diameter of about 630 nm (coincident with the reduced diameter of polystyrene nanospheres used as hard mask in the lithographic process) is observed. It is worth noting that the nanodisk contour is well defined, not notched or damaged, indicating that the lithography assisted by polystyrene nanospheres is a viable alternative to conventional ones (e.g. optical or electron).

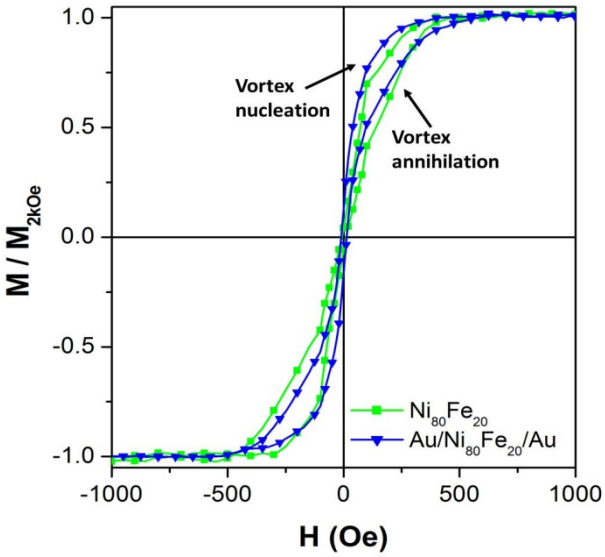

Figure 3. Room-temperature hysteresis loops of samples dispersed in deionized water: (green line) bare $Ni_{80}Fe_{20}$ nanodisks; (blue line) Au-coated $Ni_{80}Fe_{20}$ nanodisks.

The normalized room-temperature hysteresis loops measured both on bare and Au-coated $Ni_{80}Fe_{20}$ nanodisks dispersed in water are shown in Fig. 3. As expected, the magnetization reversal of bare NDs (green line) is typical of a magnetic vortex behavior [24,30]. The loop exhibits a magnetic remanence close to zero and an almost linear behavior at low fields followed by an increase of hysteresis at fields preceding the magnetic saturation. In particular, the low-field reversible linear behavior corresponds to the movement of magnetic vortex perpendicular to the applied field across the ND. Furthermore, increasing the field beyond a certain field value (annihilation field (H_{an})), the magnetic vortex gets annihilated and the magnetization reaches the saturation magnetization value M_S. Then, if the field is decreased from saturation, the magnetic vortex again nucleates at a field value (nucleation field (H_n)) lower than H_{an}. The difference between the nucleation field at decreasing field and annihilation field at increasing field is responsible for the occurring of observed hysteresis. In samples constituted by NDs in water solution, the magnetization jumps corresponding to the annihilation and nucleation of the vortex are less marked than those measured in samples consisting of dots still attached to the substrate with in-plane applied field. This smoothing of magnetization jump is due to the dispersion of NDs in water and the consequent random misalignment of their plane with respect to the applied magnetic field [16].

The magnetic vortex configuration is also observed in Au-NDs as indicated by the presence of nucleation and annihilation field in the hysteresis loop reported in Fig. 3 (blue line). As expected, the gold layer does not substantially change the magnetic behavior of the $Ni_{80}Fe_{20}$ magnetic core.

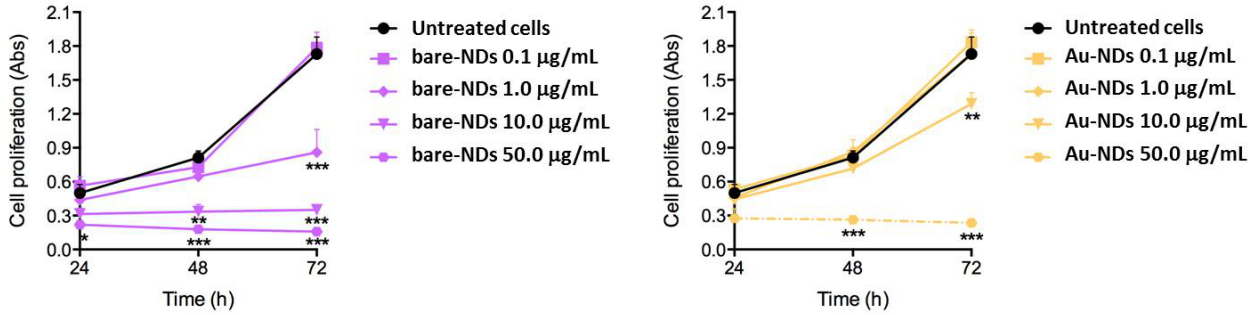

Figure 4. Effects of nanodisks with and without the protective gold layer on HT-29 cell proliferation. Cell proliferation, after exposure to increasing concentrations of nanodisks with and without the protective gold layer (0.1, 1.0, 10.0 and 50.0 µg/mL), has been evaluated at 24, 48 and 72 h by WST-1 assay. Statistical significance versus untreated cells: * $p < 0.05$, ** $p < 0.01$, *** $p < 0.001$.

As shown in Figure 4, HT-29 cells have been exposed to varying concentrations of NDs with and without the protective gold layer (from 0.1 to 50 µg/mL) in order to investigate their cytotoxicity. A dose-dependent increase in cytotoxicity has been observed after cell exposure to both nanodisk formulations. However, lower cytotoxicity has been observed over time when cells were exposed to Au-NDs compared to bare NDs, specifically 0.1 and 1.0 µg/mL Au-NDs for up to 72 h, and 10.0 µg/mL Au-NDs for up to 48 h, did not affect cell viability. Otherwise bare-NDs at 1.0 µg/ml after 72 h exposure and 10.0 µg/ml after 24 h exposure were cytotoxic. The highest nanodisk concentration (50 µg/mL) was already cytotoxic to HT-29 after 24 h incubation with bare-NDs and after 48 h incubation with Au-NDs. Therefore, it is clear that the gold layer increases the biocompatibility of disks despite the uncovered lateral surface of the dots (about 8.5 %).

Gold coating provided not only an increased biocompatibility [31] of the nanodisks but allowed easy surface modification. Thiolate groups can readily react with the gold surface and the preparation of a cysteine-fluorescein isothiocyanate (FITC) derivative has been exploited to randomly introduce fluorescence on the surface of nanodisks.

In this way, we verify the intracellular uptake of the Au-NDs at the highest nontoxic concentration, i.e. 10 µg/mL, by cytofluorimetric analysis using a FITC-conjugate. Nanodisk cellular uptake resulted to be significantly increased over time and a significant cellular uptake of Au-NDs has been observed after 24 h incubation, as shown in Figure 5.

FITC derivatized nanodisks showed superior dispersion and change in aggregation when compared to the nanodisk not derivatized.

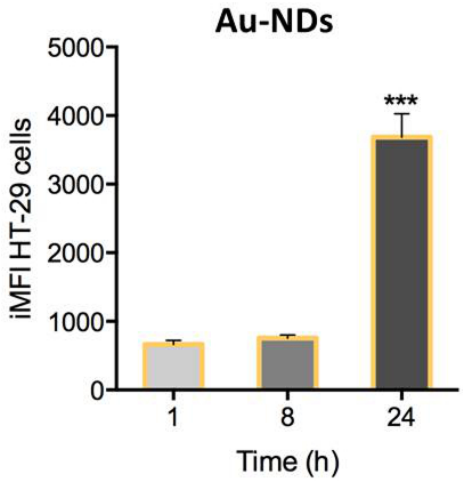

Figure5. Gold nanodisk cellular uptake. HT-29 cells have been incubated with FITC conjugated gold nanodisks (Au/Ni_{80} Fe_{20}/Au) at the same concentration (10 µg/mL) for 1, 8 and 24 h. Fluorescent signal has been detected using a flow cytometer at 488 nm excitation to measure intracellular nanodisks and expressed as the integrated median fluorescence intensity (iMFI) calculated as reported in Materials and Methods. Statistical significance versus untreated cells: *** $p < 0.001$

Conclusions

In this work, a self-assembling process based on nanospheres lithography is proposed to fabricate bare and Au-coated $Ni_{80}Fe_{20}$ nanodisks. Such a parallel process comes out as an easy-to-use, fast and low-cost method to nanostructure thin films. It allows to fabricate nanodisks at an higher rate compared to conventional, sequential nanolithography process having a well defined contour. The magnetization process of all the nanodisks is characterized by the presence of a vortex pointing to a possible exploitation in drug-delivery process and also in magnetic hyperthermia. Finally, cytoxicity text confirms that Au-coated nanodisks display an improved biocompatibility with respect to the bare ones despite the not complete coverage of the nanodisks. The intracellular uptake of the nanodisks has been confirmed by cytofluorimetric analysis using the FITC-conjugate on suface Au-coated of nanodisks.

References

1. Pankhurst QA, Connolly J, Jones SK, Dobson J. 2003 Applications of magnetic nanoparticles in biomedicine. *J. Phys. D Appl. Phys.* **36**, R167-R181.
2. Nguyen TKT. 2012 Magnetic Nanoparticles From Fabrication to Clinical Applications. CRC Press Taylor & Francis Group.
3. Kang K, Choi J, Nam JH, Lee SC, Kim KJ, Lee S-W, Chang JH. 2009 Preparation and characterization of chemically functionalized silica-coated magnetic nanoparticles as a DNA separator. *J. Phys. Chem. B* **113**, 536–543 (doi: 10.1021/jp807081b)
4. Lu C-W, Hung Y, Hsiao J-K, Yao M, Chung T-H, Lin Y-S, Wu S-H, Hsu S-C, Liu H-M, Mou C-Y, et al. 2007 Bifunctional magnetic silica nanoparticles for highly efficient human stem cell labeling. *Nano Lett.* **7**, 149–154 (doi: 10.1021/nl0624263)
5. Sun C, Lee JSH, Zhang M. 2008 Magnetic nanoparticles in MR imaging and drug delivery. *Adv. Drug Deliver Rev.* **60**, 1252-1265 (doi:10.1016/j.addr.2008.03.018)

6. Dutz S, Hergt R. 2014 Magnetic particle hyperthermia – a promising tumor therapy? *Nanotechnology* **25**, 28pp (doi: 10.1088/0957-4484/25/45/452001)
7. Lu A-H, Salabas EL, Schuth F. 2007 Magnetic nanoparticles: synthesis, protection, functionalization, and application. *Angew. Chem. Int. Edit*. **46**, 1222-1244. (doi: 10.1002/anie.200602866)
8. Ito A, Shinkai M, Honda H, Kobayashic T. 2005 Medical application of functionalized magnetic nanoparticles. *J. Biosci. Bioeng.* **100**, 1-11 (doi:10.1263/jbb.100.1)
9. Tamer U, Gundogdu Y, Boyaci IH, Pekmez K. 2009 Synthesis of magnetic core–shell Fe_3O_4–Au nanoparticle for biomolecule immobilization and detection *J. Nanopart. Res.* **12**, 1187-1196. (doi: 10.1007/s11051-009-9749-0)
10. Cho S-J, Idrobo J-C, Olamit J, Liu K, Browning ND, Kauzlarich SM. 2005 Growth mechanisms and oxidation resistance of gold-coated iron nanoparticles *Chem. Mater.* **17**, 3181-3186. (doi: 10.1021/cm0500713)
11. Yu H, Chen M, Rice PM, Wang SX, White RL, Sun S. 2005 Dumbbell-like bifunctional Au−Fe_3O_4 nanoparticles *Nano Lett.* **5**, 379-382. (doi: 10.1021/nl047955q)
12. Wang L, Luo J, Maye MM, Fan Q, Rendeng Q, Engelhard MH, Wang C, Lin Y, Zhong C-J, 2005 Iron oxide–gold core–shell nanoparticles and thin film assembly *J. Mater. Chem.* **15**, 1821-1832. (doi: 10.1039/B501375E)
13. Caruntu D, Cushing BL, Caruntu G, O'Connor J. 2005 Attachment of Gold Nanograins onto Colloidal Magnetite Nanocrystals *Chem. Mater.* **17**, 3398-3402. (doi: 10.1021/cm050280n)
14. Tartaj P, del Puerto Morales M, Veintemillas-Verdaguer S, González-Carreño T, Serna CJ. 2003 The preparation of magnetic nanoparticles for applications in biomedicine *J. Phys. D: Appl. Phys.* **36**, R182-R197.
15. Hasany SF, Ahmed I, Rajan J, Rehman A. 2012 Systematic review of the preparation techniques of iron oxide magnetic nanoparticles *Nanosci. Nanotechnol.* **2**, 148-158. (doi: 10.5923/j.nn.20120206.01)
16. Tiberto P, Barrera G, Celegato F, Conta G, Coïsson M, Vinai F, Albertini F. 2015 $Ni_{80}Fe_{20}$ nanodisks by nanosphere lithography for biomedical applications *J. Appl. Phys.* **117**, 17B304-1-17B304-4. (doi: 10.1063/1.4913278)
17. Hu W, Wilson RJ, Koh A, Fu A, Faranesh AZ, Earhart CM, Osterfeld SJ, Han S-J, Xu L, Guccione S, et al. 2008 High-moment antiferromagnetic nanoparticles with tunable magnetic properties *Adv. Mater.* **20**, 1479-1483. (doi: 10.1002/adma.200703077)
18. Joisten H, Courcier T, Balint P, Sabon P, Faure-Vincent J, Auffret S, Dieny B. 2010 Self-polarization phenomenon and control of dispersion of synthetic antiferromagnetic nanoparticles for biological applications *Appl. Phys. Lett.* **97**, 253112-1-253112-3. (doi: 10.1063/1.3518702)
19. Kosiorek A, Kandulski W, Glaczynska H, Giersig M. 2005 Fabrication of nanoscale rings, dots, and rods by combining shadow nanosphere lithography and annealed polystyrene nanosphere masks *Small* **1**, 439-444. (doi: 10.1002/smll.200400099)
20. Cheng JY, Ross CA, Chan VZ-H, Thomas EL, Lammertink RGH, Vancso GJ. 2001 Formation of a cobalt magnetic dot array via block copolymer lithography *Adv. Mater.* **13**, 1174-1178. (doi: 10.1002/1521-4095(200108)13:15<1174::AID-ADMA1174>3.0.CO;2-Q)
21. Decuzzi P, Ferrari M. 2006 The adhesive strength of non-spherical particles mediated by specific interactions *Biomaterials* **27**, 5307-5314. (doi:10.1016/j.biomaterials.2006.05.024)
22. Gentile F, Chiappini C, Fine D, Bhavane RC, Peluccio MS, Ming-Cheng Cheng M, Liu X, Ferrari M, Decuzzi P. 2008 The effect of shape on the margination dynamics of non-neutrally buoyant particles in two-dimensional shear flows *J. Biomech.* **41**, 2312-2318. (doi:10.1016/j.jbiomech.2008.03.021)

23. Decuzzi P, Godin B, Tanaka T, Lee S-Y, Chiappini C, Liu X, Ferrari M. 2010 Size and shape effects in the biodistribution of intravascularly injected particles *J. Control. Release* **141**, 320-327. (doi: doi:10.1016/j.jconrel.2009.10.014)
24. Coey JMD. 2009 Magnetism and Magnetic Materials Cambridge University Press.
25. Leulmi S, Chauchet X, Morcrette M, Ortiz G, Joisten H, Sabon P, Livache T, Hou Y, Carrière M, Lequiena S, Dieny B. 2015 Triggering the apoptosis of targeted human renal cancer cells by the vibration of anisotropic magnetic particles attached to the cell membrane *Nanoscale* **7**, 15904-15914. (doi: 10.1039/c5nr03518j)
26. Kim D-H, Rozhkova EA, Ulasov IV, Bader SB, Rajh T, Lesniak MS, Novosad V. 2009 Biofunctionalized magnetic-vortex microdiscs for targeted cancer-cell destruction *Nat. Mater.* **9** 165-171. (doi:10.1038/nmat2591)
27. Issa B, Obaidat IM, Albiss BA, Haik Y. 2013 Magnetic nanoparticles: surface effects and properties related to biomedicine applications *Int. J. Mol. Sci.* **14**, 21266-21305. (doi: :10.3390/ijms141121266)
28. Chen Y, 2015 Nanofabrication by electron beam lithography and its applications: A review *Microelectron. Eng.* **135**, 57-72. (doi: 10.1016/j.mee.2015.02.042)
29. Weekes SM, Ogrin FY, Murray WA, Keatley PS. 2007 Macroscopic arrays of magnetic nanostructures from self-assembled nanosphere templates *Langmuir*g **23**, 1057-1060. (doi: 10.1021/la061396g)
30. Cowburn RP, Koltsov DK, Adeyeye AO, Welland ME. 1999 Single-Domain Circular Nanomagnets *Phys. Rev. Lett.* **85,** 1042-45. (doi: 10.1103/PhysRevLett.83.1042)
31. Nel A, Mädler L, Velegol D, Xia T, Hoek EMV, Somasundaran P, Klaessig F, Castranova V, Thompson M. 2009 Understanding biophysicochemical interactions at the nano-bio interface. *Nat. Mater*. **8**, 543-557. (doi: 10.1038/nmat2442)